Electronic Supplementary Material (ESI) for Nanoscale.
This journal is © The Royal Society of Chemistry 2024

Electronic Supplementary Information

Exploring ssDNA translocation through α-hemolysin using Coarse-Grained Steered Molecular Dynamics†

Cagla Okyay,[a] Delphine Dessaux,[a‡], Rosa Ramirez,[a] Jérôme Mathé,[a] and Nathalie Basdevant*[a]

Experimental measurement of the translocation time of ssDNA in α-Hemolysin

The experiments were performed under the conditions exposed in the Methods Section 4.1. The current is recorded using an amplifier Axon Multiclamp 700B (Molecular device, USA), low-pass filtered by a four-pole Bessel filter with a cutoff frequency of 50 kHz (Khron-Hite, USA). It is then digitized at a sampling frequency of 1 MHz using a 16-bit acquisition card (National Instruments, Austin, TX) and finally saved directly to the hard drive of a computer. The acquisition card is controlled via a homemade program written with LabView (National Instruments).

The events were detected and their characteristics measured using a current-threshold (Th) method described in earlier papers (*e.g.* see ref[1]) using in-house Python 3 routines. The scatter plot of Fig. S1 is a common representation of the results. We computed the density of events in the current-Log(time) space and fit it as a double 2D-Gaussian curve. The fitting procedure gave 2 peaks with different translocation times (T_t) and residual currents (I_b): the 3' one at $T_t = 3.2 \pm 0.2$ μs and $I_b = 9.4 \pm 0.4$ % and the 5' one at $T_t = 7.1 \pm 0.4$ μs and $I_b = 13.1 \pm 0.9$ %. This probability density was used with a Monte Carlo algorithm to distribute the events between the two type of events. The result of the MC algorithm is displayed on Fig. S1 using colors. The translocation time ratio of 5' compared to 3' translocation is then 2.22.

[a] *Université Paris-Saclay, Univ Evry, CY Cergy Paris Université, CNRS, LAMBE, 91025, Évry-Courcouronnes, France.*
* *corresponding author: nathalie.basdevant@univ-evry.fr*
‡ Present address: TBI, Université de Toulouse, CNRS, INRAE, INSA, Toulouse, France

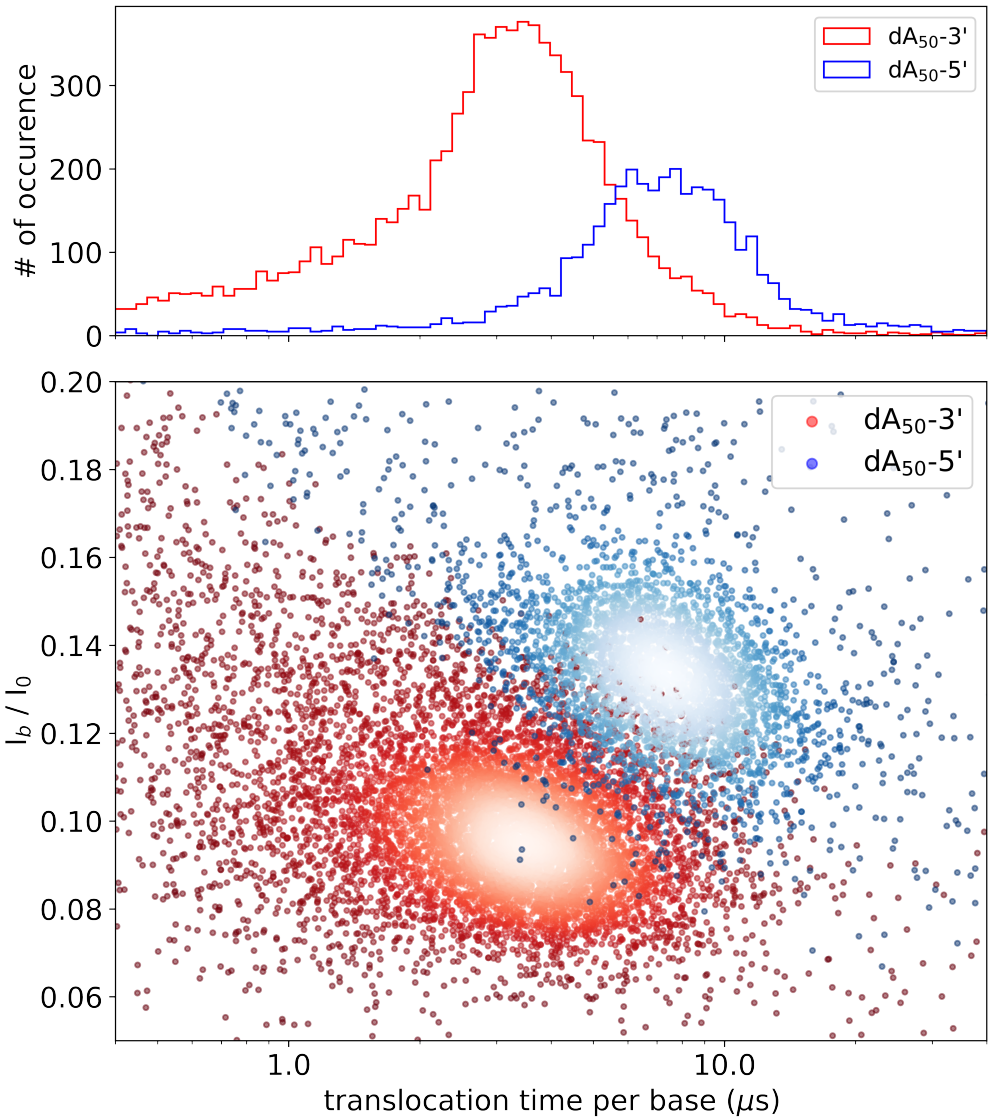

Fig. S1 Upper figure shows the experimental translocation time per base distribution for poly(dA)$_{50}$ with the α-hemolysin nanopore at 120 mV and room temperature. The distribution is obtained by dividing the translocation time per molecule by the number of nucleotides (50). In the lower figure is represented the scatter plot of events: each dot represents an event (about 12,500 events on this plot) with its time of translocation (per base) and the level of blockage (I_b/I_0 with I_0 the open pore current and I_b residual current or blocked current when the molecule is translocating through the pore). Both current and time are distinguishable between 3' oriented and 5' oriented ssDNA molecules. The separation of the 3' and 5' events was done using a Monte Carlo algorithm with the event bimodal probability density in the current-time space of the cloud of events.

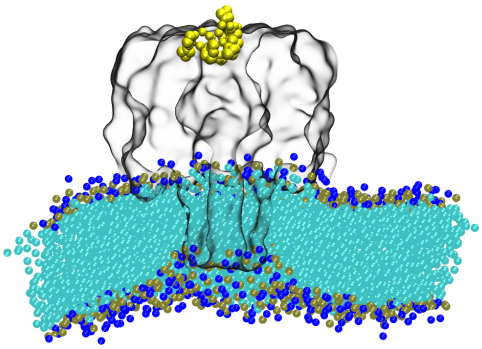

Fig. S2 ssDNA translocation simulation for a polyA DNA molecule of 10 nucleotides in the presence of an external electric field of 0.03 V/nm (equivalent to an electric potentiel difference of approximately 800 mV). The applied electric field is not sufficient to drive the ssDNA molecule through the nanopore and ssDNA molecule interacts with the cap of the nanopore. Snapshot is taken after 500 ns.

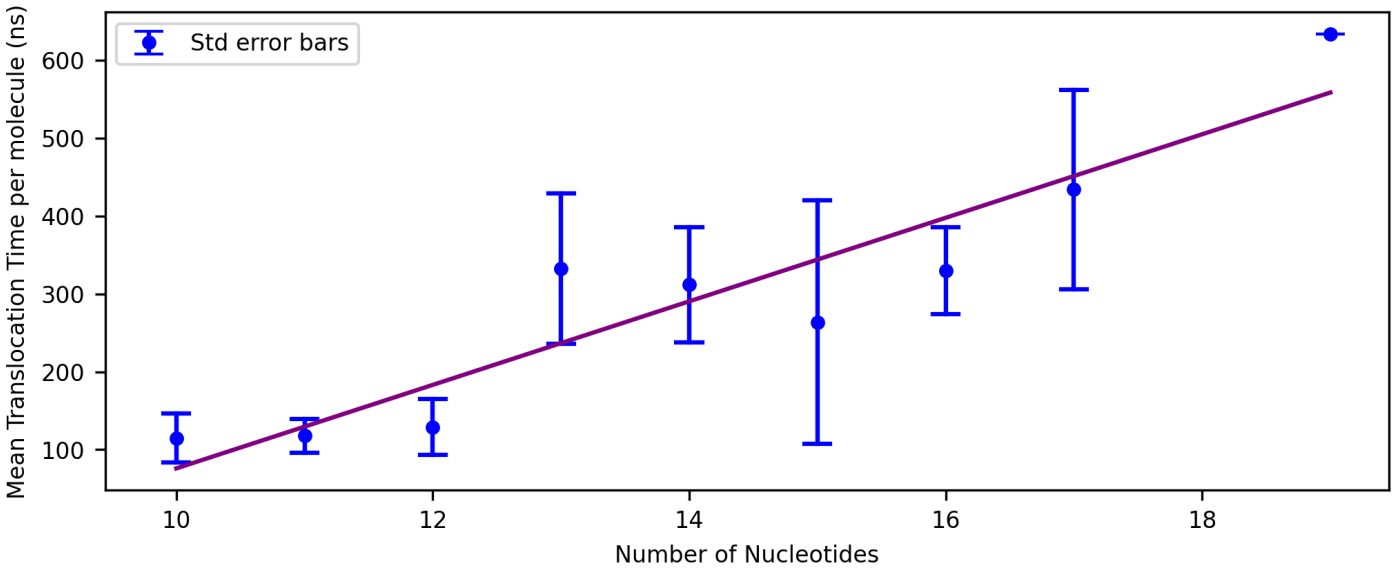

Fig. S3 Effect of ssDNA length on translocation time per molecule in cf-SMD simulations. Average translocation time per molecule is given for each system, standard error is shown as error bars. Linear regression indicated by purple line. No data is available for 18-nucleotide poly(dA) and only one total translocation event was observed for 19-nucleotide poly(dA).

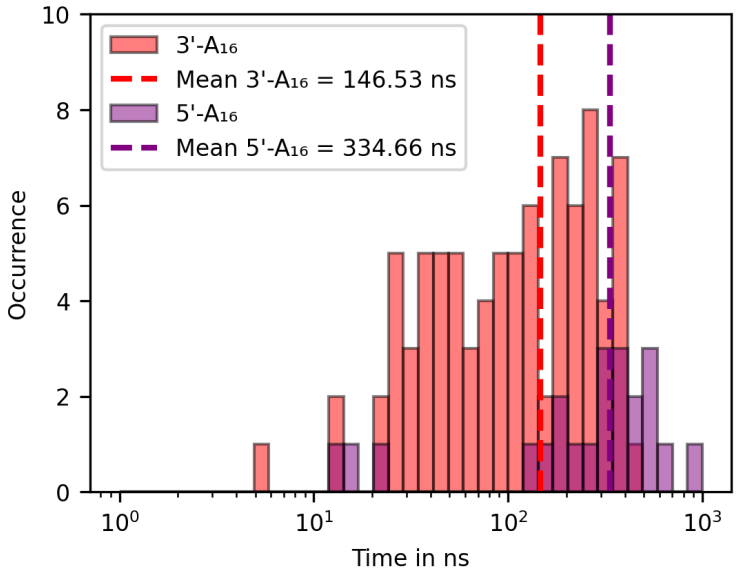

Fig. S4 The effect of orientation of the DNA molecule at the pore entrance on translocation time per base distribution in CG cf-SMD simulations. Distribution is given on a logarithmic scale. The averages of translocation time per base for both 3' and 5' strand orientations are indicated by red and purple dashed lines, respectively.

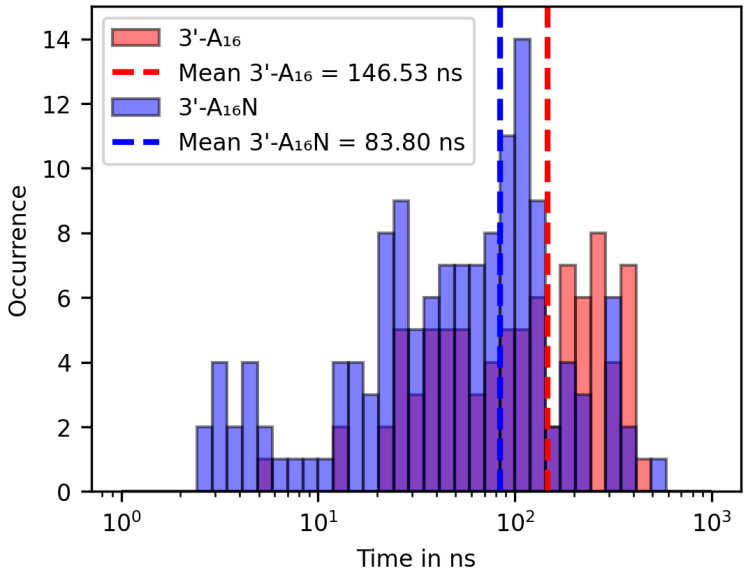

Fig. S5 The effect of DNA charges on translocation time per base distribution in CG cf-SMD simulations. Distribution is given on a logarithmic scale. The averages of translocation time per base for both charged and neutral strands are indicated by red and blue dashed lines, respectively.

We calculated the mean radius by considering all the residues of the constriction (E111/K147) and the bottom (D127/K131) rings pointing inwards. The center of mass was calculated for each group of residues on the seven chains of α-hemolysin, and the center of mass of all seven groups was also determined. Subsequently, the distance between the center of mass of each group and the global center of mass of all groups was calculated. The mean value of these distances represents the mean radius.

Table S1 Mean radius of constriction (E111/K147) and bottom (D127/K131) rings during ssDNA translocation simulations of 3'-A_{16} and 3'-A_{16}N systems (standard error is given).

System	Ring	Mean radius in nm	
		sim. #1	sim. #2
3'-A_{16}	E111/K147	1.04 ± 0.02	1.03 ± 0.02
	D127/K131	1.22 ± 0.03	1.22 ± 0.04
3'-A_{16}N	E111/K147	1.05 ± 0.02	1.06 ± 0.02
	D127/K131	1.22 ± 0.03	1.26 ± 0.03

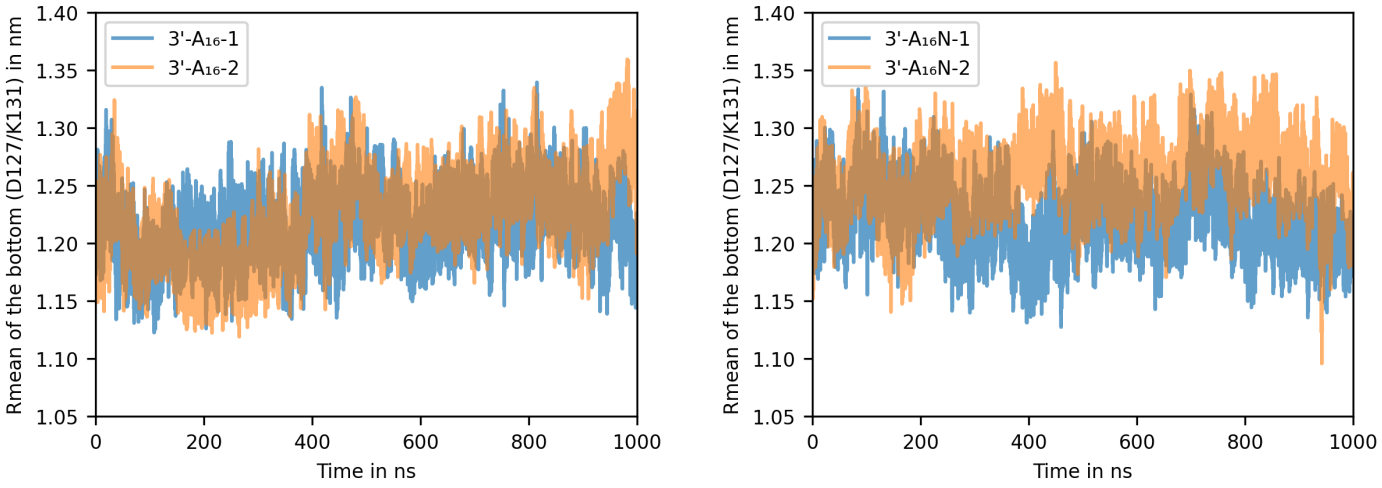

(a) Mean radius of the bottom (D127/K131) ring during 1 μs MD simulation of both replicas of 3'-A_{16} system.

(b) Mean radius of the bottom (D127/K131) ring during 1 μs MD simulation of both replicas of 3'-A_{16}N system.

Fig. S6 The effect of DNA charges on the evolution of the mean radius of the bottom ring (D127/K131).

Table S2 Number of contacts between ssDNA of 3'-A_{16} and of 3'-A_{16}N systems with constriction (E111/K147) and bottom (D127/K131) rings in the stem during complete translocation events for each replica.

System	sim. #	Ring	T#1	T#2	T#3	T#4	T#5
3'-A_{16}	1	E111/K147	126,933	75,569	192,116		
		D127/K131	115,882	67,343	155,697		
	2	E111/K147	226,842	247,202			
		D127/K131	246,282	197,655			
3'-A_{16}N	1	E111/K147	24,701	40,546	64,415		
		D127/K131	20,954	39,765	76,030		
	2	E111/K147	34,006	100,186	46,795	17,658	43,995
		D127/K131	34,803	105,316	35,107	13,023	17,111

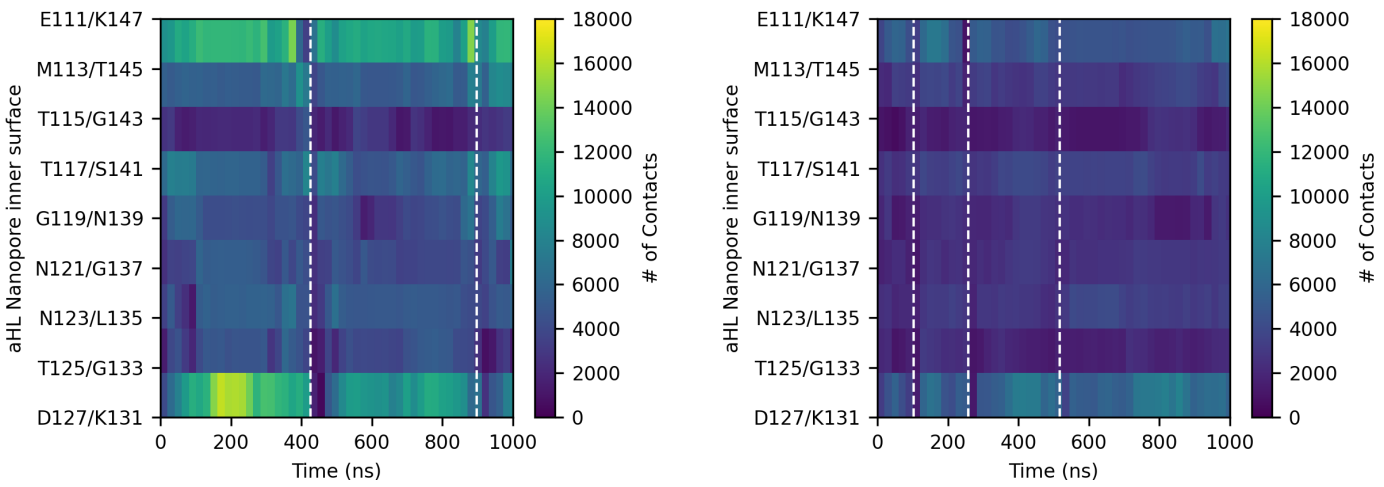

(a) Contact map of 3'-A_{16}-2 with each ring in the stem during 1 μs MD simulation. Dashed lines show the end of each translocation event.

(b) Contact map of 3'-A_{16}N-1 with each ring in the stem during 1 μs MD simulation. Dashed lines show the end of each translocation event.

Fig. S7 Contact maps between ssDNA and αHL during 3'-A_{16}-2 and 3'-A_{16}N-1 simulations.

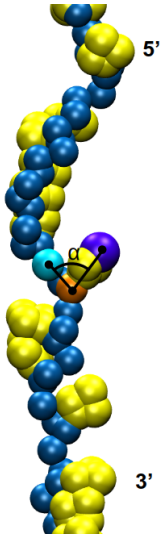

Fig. S8 Representation of the tilt angle defined between the center of mass of BB1, BB3 and SC3 beads of the ssDNA molecule, represented in cyan, orange and purple beads respectively. 5' and 3' extremities are indicated on the illustration.

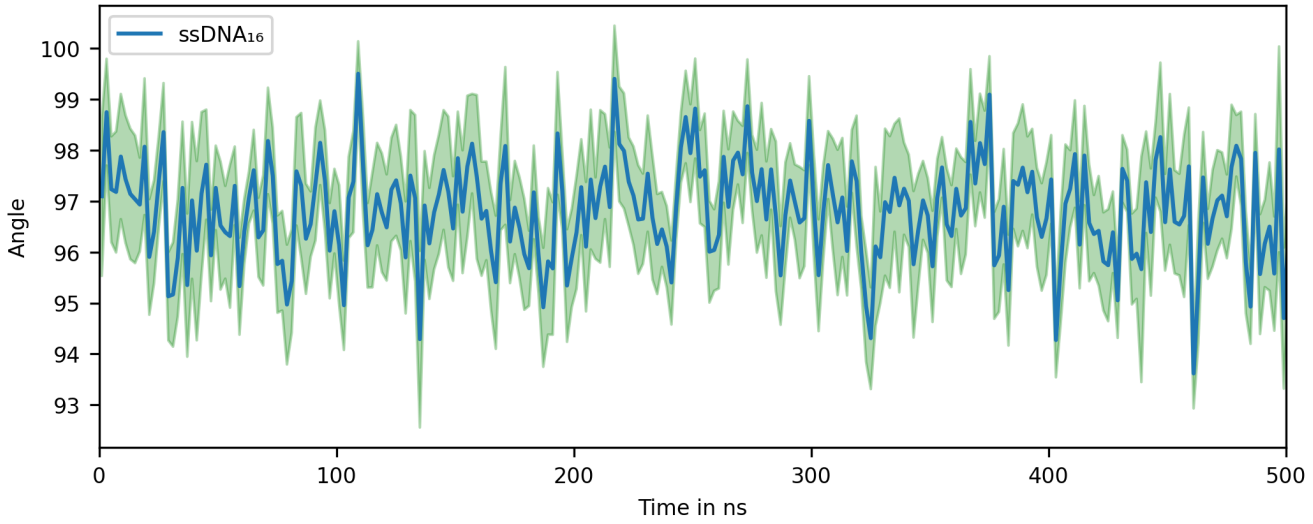

Fig. S9 Average tilt angles of DNA bases relative to the backbone for 16-nucleotide poly(dA) molecule free in the solution. Standard error is given in green.

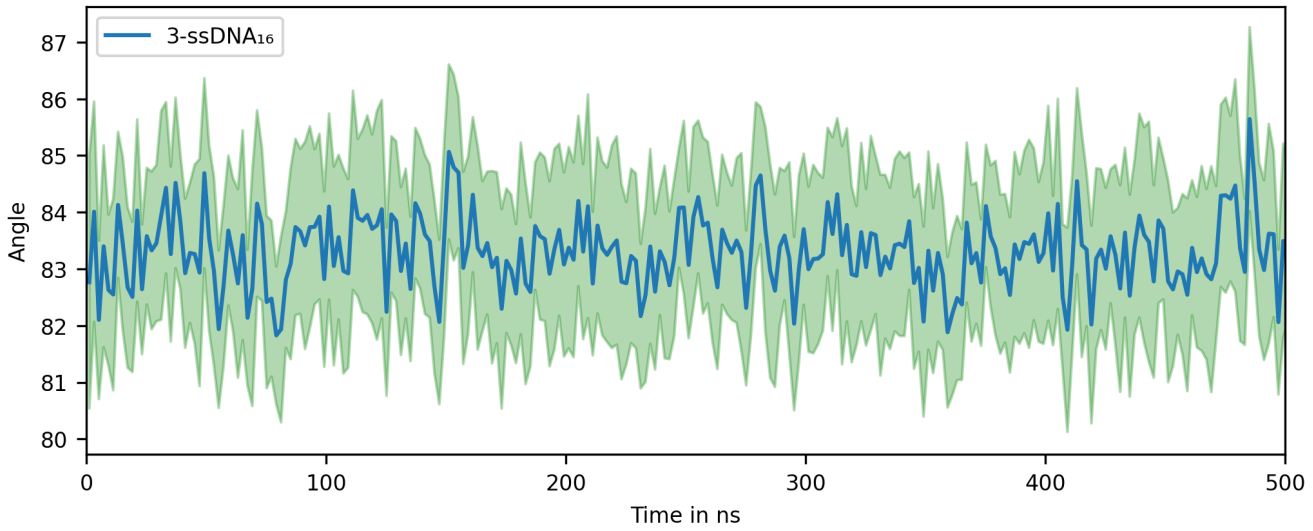

Fig. S10 Average tilt angles of DNA bases relative to the backbone for 16-nucleotide poly(dA) molecule pulled by their 3' end in the absence of the nanopore. Standard error is given in green.

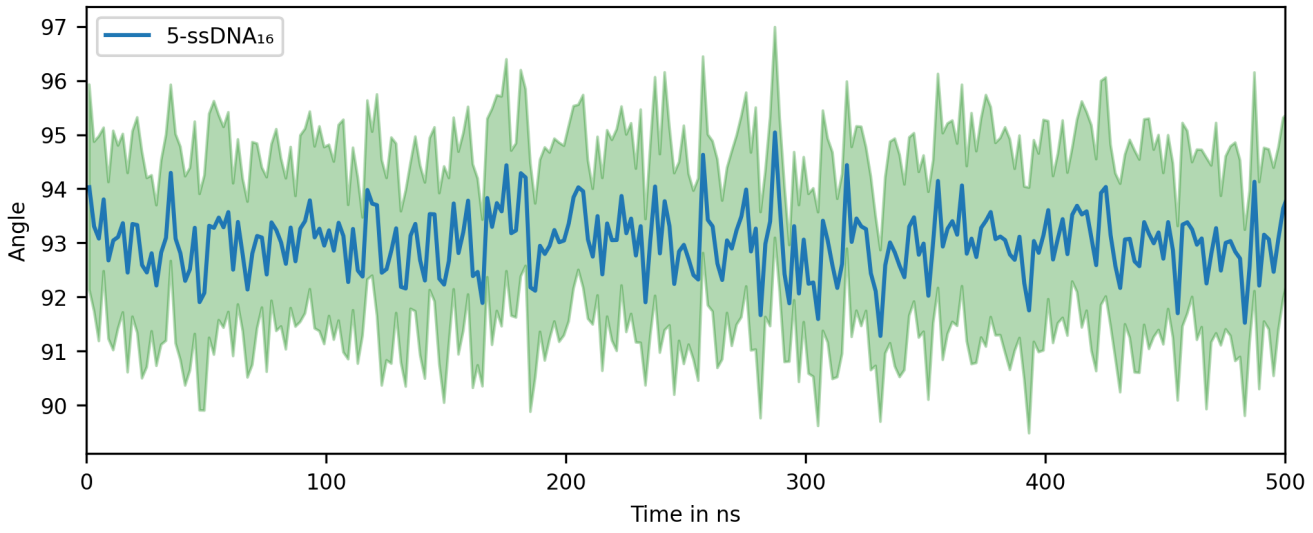

Fig. S11 Average tilt angles of DNA bases relative to the backbone for 16-nucleotide poly(dA) molecule pulled by their 5' end in the absence of the nanopore. Standard error is given in green.

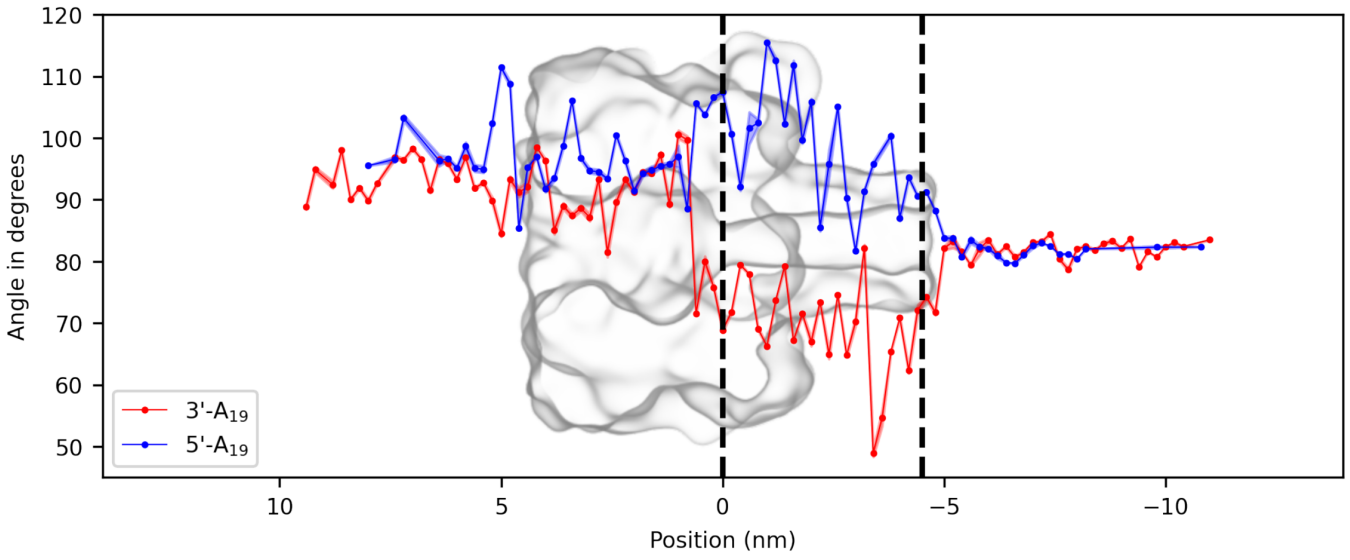

Fig. S12 Effect of ssDNA orientation at the pore entrance on tilt angles during translocation. Average tilt angles of DNA bases relative to the backbone for 3' end and 5' end oriented 19-nucleotide poly(dA) molecules are given as red and blue circles, as a function of positions in z-direction inside the simulation box. The displayed values represent the mean tilt angle for the 18 bases (excluding bases at both extremities) across all translocation events in the two simulation replicas, accompanied by their standard error. The black dashed lines denote the constriction and bottom of the stem.

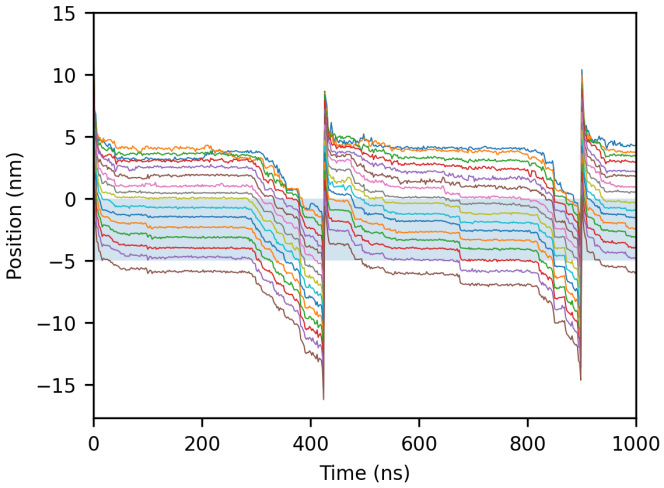

(a) Base positions of 3'-A_{16}-2 in the z-direction. The stem is depicted as a blue-filled region, with 0 on the z-axis corresponding to the pore constriction.

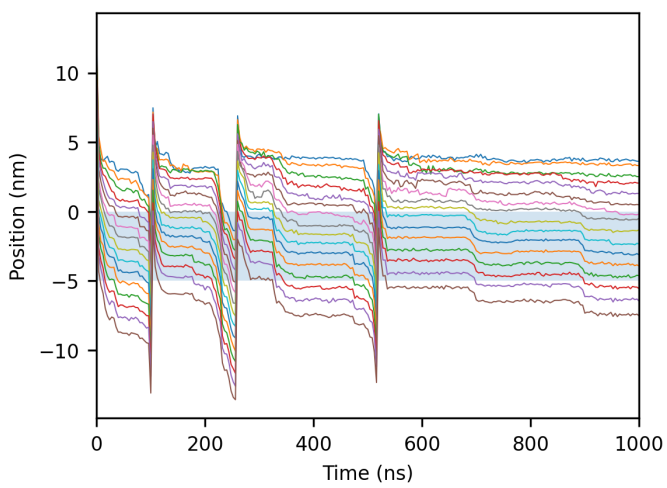

(b) Base positions of 3'-A_{16}N-1 in the z-direction. The stem is depicted as a blue-filled region, with 0 on the z-axis corresponding to the pore constriction.

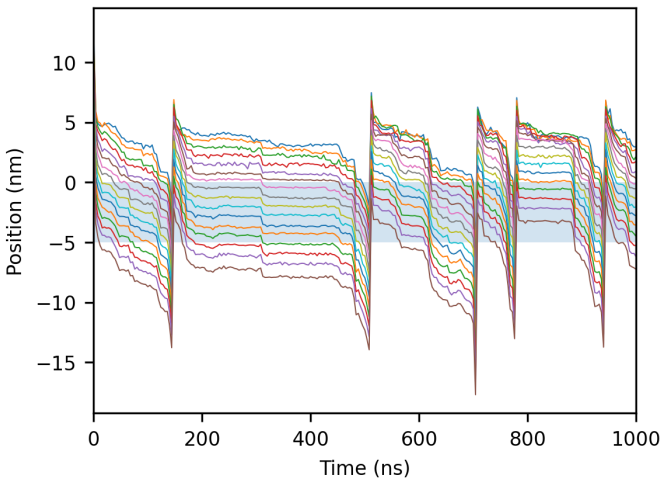

(c) Base positions of 3'-A_{16}N-2 in the z-direction. The stem is depicted as a blue-filled region, with 0 on the z-axis corresponding to the pore constriction.

(d) Legend for the plots, each color indicating a base number

Fig. S13 Evolution of the base positions in z-direction of 3'-A_{16} systems.

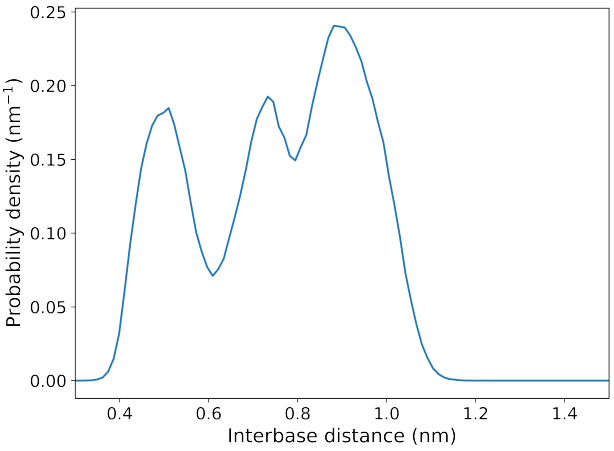

(a) Probability density of inter-base distance for a A_{16} ssDNA free in solution. We observe 3 main conformations at 0.50 ± 0.08 nm, 0.71 ± 0.08 nm and 0.91 ± 0.12, which are coexisting along the chain.

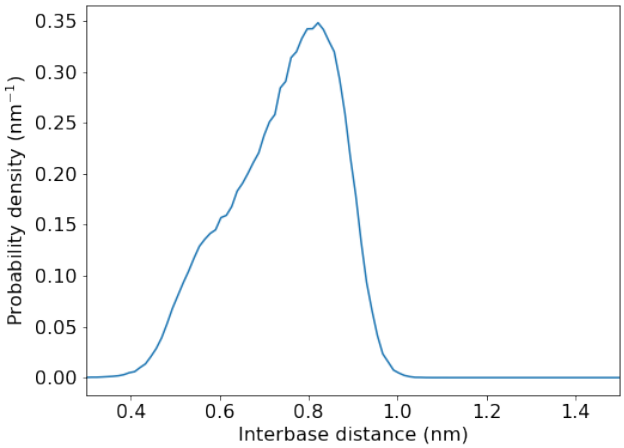

(b) Probability density of inter-base distance for a 3'-A_{16} ssDNA pulled by the SMD force in solution (in the absence of the pore). We observe one main conformation at 0.88 ± 0.11 nm and a minor one at 0.55 ± 0.15 nm.

Fig. S14 Inter-base distance observed in two control simulations: ssDNA free in solution and ssDNA dragged in solution by the pulling force from 3' end.

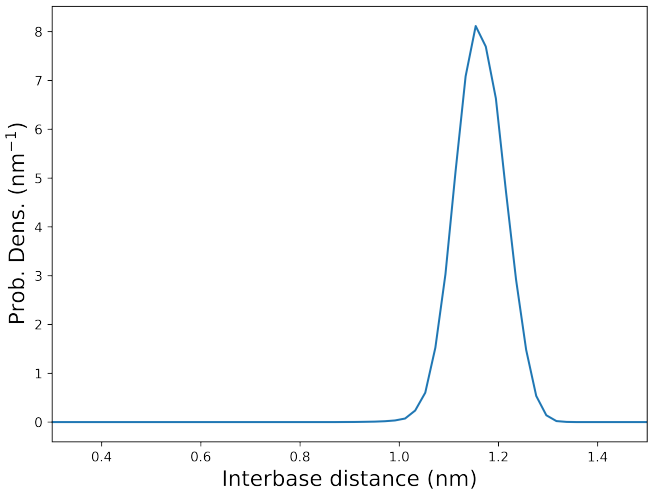

Fig. S15 Inter-base distance of the first pair of bases for 3'-A_{16} simulations. As the SMD force is applied to the first base, this inter-base is overstretched.

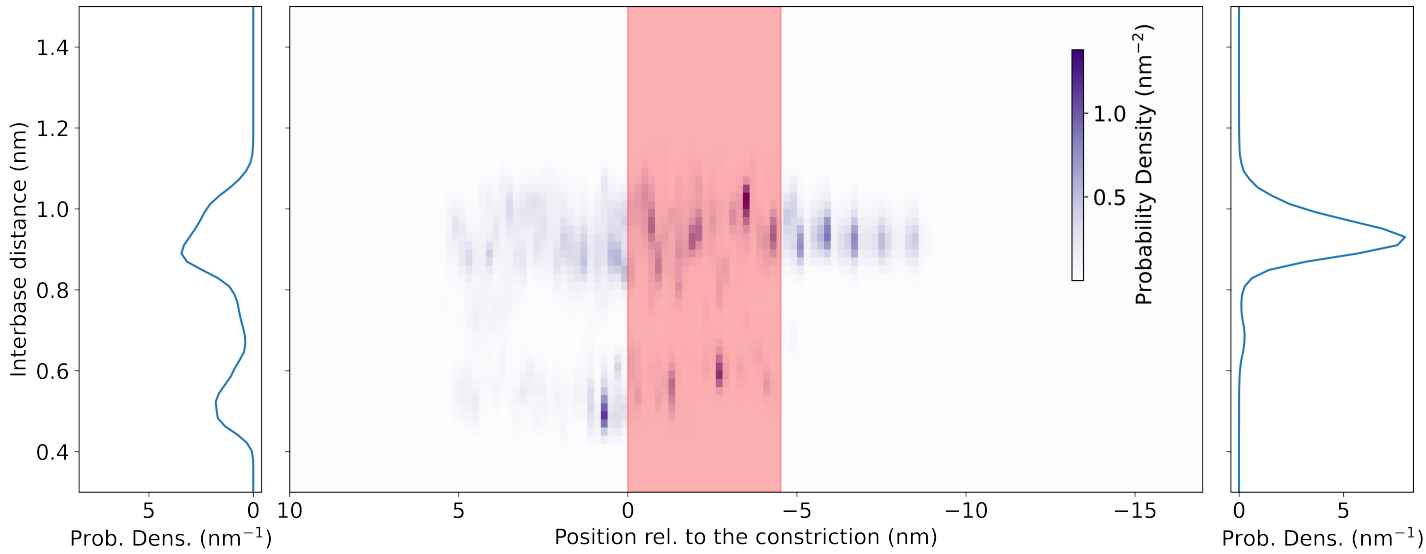

Fig. S16 Inter-base distances for 5'-A_{16} simulations. The distance between two consecutive bases (inter-base distance) for all pairs except for the first and last one are represented as a probability density. Central panel: probability density of inter-bases distance as a function of the position along the pore axis. The stem is depicted as a red-filled region, with 0 on the z-axis corresponding to the pore constriction ring (E111/K147). Left panel: probability density of inter-bases distance before the entry of the ssDNA in the stem. It is the integration of the central panel over the position above the stem ($z > z_{\text{constriction}} = 0$ nm). Right panel: probability density of inter-bases distance after the exit of the DNA from the stem. It is the integration of the central panel over the position below the stem ($z < z_{\text{bottom}} \simeq -4.5$ nm)

Table S3 Entry angle and distance of ssDNA molecules in initial structures.

System name	Entry angle (°)	Distance (nm)
3'-A_{10}	4.56	5.41
3'-A_{11}	9.57	5.46
3'-A_{12}	8.47	5.06
3'-A_{13}	4.30	4.47
3'-A_{14}	2.35	4.73
3'-A_{15}	7.45	5.32
3'-A_{16}	6.51	4.70
3'-A_{16}N	9.69	3.86
5'-A_{16}	8.92	4.94
3'-A_{17}	0.83	5.23
3'-A_{18}	2.28	5.11
3'-A_{19}	5.04	5.02

Notes and references

1 P. Bayat, C. Rambaud, B. Priem, M. Bourderioux, M. Bilong, S. Poyer, M. Pastoriza-Gallego, A. Oukhaled, J. Mathé and R. Daniel, *Nature Communications*, 2022, **13**, 5113.